Dynamic melting of confined vortex matter

Besseling, R.; Kokubo, N.; Kes, P.H.

Dynamic Melting of Confined Vortex Matter

R. Besseling, N. Kokubo, and P. H. Kes
Kamerlingh Onnes Laboratorium, Leiden University, P.O. Box 9504, 2300 RA Leiden, the Netherlands
(Received 10 February 2003; published 24 October 2003)

We study *dynamic* melting of confined vortex matter moving in disordered, mesoscopic channels by mode-locking experiments. The dynamic melting transition, characterized by a collapse of the mode-locking effect, strongly depends on the frequency, i.e., on the average velocity of the vortices. The associated dynamic ordering velocity diverges upon approaching the equilibrium melting line $T_{m,e}(B)$ as $v_c \sim (T_{m,e} - T)^{-1}$. The data provide the first direct evidence for velocity dependent melting and show that the phenomenon also takes place in a system under disordered confinement.

DOI: 10.1103/PhysRevLett.91.177002 PACS numbers: 74.25.Qt, 64.60.Ht, 64.70.Dv, 83.50.Ha

An intriguing aspect of periodic media driven through a (random) pinning potential, e.g., vortex lattices (VLs) in superconductors [1], charge density waves (CDWs) [2], or conventional sliding solids [3], is the possibility of a dynamic ordering (DO) transition [4,5]: While at a small velocity, pinning may disrupt the lattice, causing liquid-like flow [6] around pinned islands, at large velocity the influence of pinning diminishes and the elastic interactions dominate, favoring a crystalline structure.

The DO phenomenon becomes particularly interesting close to the *thermodynamic* melting point of the medium, since in addition to fluctuations due to pinning also thermal fluctuations become relevant [5,7]. Their combined effect was first studied by Koshelev and Vinokur [5] for 2D VLs. They introduced the concept of a *shaking temperature* T_{sh}, characterizing the fluctuations in the moving frame due to the quenched disorder. This shaking diminishes with increasing velocity as $k_B T_{sh} = \Gamma_{p,v}/v$ ($\Gamma_{p,v}$ reflects the pinning strength and viscous damping). Fluidlike, incoherent motion sets in when the effective "temperature" $T + T_{sh}$ equals the equilibrium melting temperature $T_{m,e}$ of the pure system. Hence, for $T < T_{m,e}$ there exists a recrystallization velocity,

$$v_c = \Gamma_{p,v}/[k_B(T_{m,e} - T)], \qquad (1)$$

which diverges when temperature approaches $T_{m,e}$. Indications for this scenario were found in experiments on superconducting films [8] by identifying an inflection point in the current-voltage (IV) curves with DO. This identification seemed justified from simulations [9] but more direct experimental evidence for the phenomenology in [5] is still lacking. Simulations of a density gradient driven system [10] in fact suggest that the inflection point can also be due to changes in large-scale flow morphology while recent experiments on crystals [11] have shown that for a 3D VL the inflection point is due to macroscopic coexistence of two phases and not due to *microscopic* DO.

In this Letter, we study DO of *confined* vortex matter flowing in disordered mesoscopic channels using a completely different dynamic probe. In [12], we showed how a mode-locking (ML) technique can be used to explore the flow configuration in the channels in the presence of strong disorder from the vortex arrays in the channel edges. The ML phenomenon occurs due to coupling between, on the one hand, lattice modes of frequency $f_{\mathrm{int}} = qv/a$, with q an integer and a the lattice periodicity, which may exist in an array that moves coherently with velocity v, and, on the other hand, a superimposed rf drive of frequency f at an integer fraction $1/p$ of f_{int} [13]. This coupling produces plateaus in the dc-transport (IV) curves or sharp peaks in the differential conductance (dI/dV) when $v = (p/q)fa$. However, these peaks are reduced and can eventually vanish due to incoherent velocity fluctuations in the moving array, arising from both thermal and quenched disorder [14,15]. Thus, the collapse of the ML peak marks the transition from coherent to incoherent flow. Using this criterion, we provide for the first time conclusive evidence for a velocity dependent melting transition at v_c [16] and probe the divergence of v_c upon approaching the static phase boundary.

The experiments are performed on a superconducting double layer of weak pinning amorphous (a-)$Nb_{1-x}Ge_x$ ($x \simeq 0.3$, 550 nm thickness, $T_c = 2.68$ K, normal resistivity $\rho_n = 2\ \mu\Omega$ m) and strong pinning NbN (50 nm thickness) on top, containing $N_{ch}(\simeq 200)$ straight channels of width $w = 230$ nm etched to a depth of 300 nm [17]. Vortices in the channels are confined between channel edges (CEs) consisting of pinned, disordered VLs which impose both a periodic and random potential on the confined vortices via their mutual shear interaction, characterized by a shear modulus c_{66}. This potential determines both the threshold force density $F_p \propto c_{66}/w$ and the dynamics of vortices in the channel [12,18,19]. We measured dc and dc-rf transport versus magnetic field and temperature using a four probe configuration. The sample was immersed in superfluid ^{4}He. The frequency of the applied rf current was in the range 1–200 MHz, its amplitude I_{rf} could be as large as 2 mA [20].

Because of the confinement, the ML condition for channel flow attains a particularly useful form: Although the array in the channel may be frustrated, meaning that the average longitudinal periodicity $a \neq a_0$ and the row spacing $b \neq b_0$ ($a_0 = 2b_0/\sqrt{3} \simeq 1.075\sqrt{\Phi_0/B}$ are the equilibrium values), the *voltage* at which the main interference ($p = q = 1$) occurs is simply given by [12]

$$V_{1,1} = \Phi_0 f n N_{ch}, \tag{2}$$

with n is the number of moving rows in each channel.

We first discuss the typical behavior in the solid phase where matching effects between the confined array and the channel width dominate the behavior. In Fig. 1, the thick line shows the dc-depinning force density $F_p = J_p B$ ($I_{\rm rf} = 0$). For fields $B \lesssim 1.1$ T two oscillations in F_p are seen. The inset shows dI/dV curves in the presence of an 85 MHz rf current ($I_{\rm rf} = 0.53$ mA) versus voltage for fields 0.9 T $\leq B \leq$ 1.16 T. The data for 0.9 T exhibits a peak in dI/dV corresponding to ML of seven vortex rows in each channel. For larger fields, the amplitude of this peak decays while another peak, corresponding to eight rows, appears. The field region where these peaks coexist (0.92 T $\lesssim B \lesssim$ 1 T) evidently corresponds to the situation of maximum mismatch between the natural width nb_0 of $n = 7, 8$ vortex rows and the effective channel width (estimated as $w_{\rm eff} = 315$ nm). In the same field regime F_p exhibits a maximum. As shown in [12], this maximum at mismatch is caused by jamming of the flow at locations in the channel where the number of rows switches from n to $n \pm 1$. The motion there is partially blocked by dislocations with Burgers vectors that are almost perpendicular to the flow direction. The structural disorder of the fixed VL in the CEs is responsible for this phenomenon.

We now turn to the behavior in larger magnetic fields, $B \gtrsim 1.1$ T. At $B \simeq 1.15$ T, F_p shows a rapid decrease after a small upturn. This drop coincides with the onset of a measurable zero-bias resistance R_0 (displayed on the right axis). These two distinct features reflect the loss of shear rigidity of the vortex configuration inside the channel, indicating a transition to a confined vortex liquid [17]. Note that these features occur well below the magnetic field at which the transition from $n = 8$ to 9 vortex rows is expected from the condition $8.5b_0 = w_{\rm eff}$, namely $B_{8,9} = 1.27$ T. In addition, neither F_p nor R_0 show any particular features at $B_{8,9}$, which shows that the liquid is insensitive to (mis)matching effects.

The ML experiments provide important new information regarding the coherence and the shear rigidity of the *moving* array. Figure 2(a) shows dI/dV data in the field range 1.14–1.3 T plotted versus the normalized voltage for a 6 MHz rf current. The ML peak in the upper curve ($B =$ 1.14 T) corresponds to the coherent motion of eight rows. For a larger field, the peak amplitude drops rapidly and vanishes at $B \simeq 1.2$ T. Above 1.2 T, the dI/dV versus V curves remain featureless. The vanishing of the ML signal marks the transition from coherent motion of a vortex solid to incoherent "liquid" motion. A similar interpretation of this phenomenon was suggested in [14] with respect to the VL melting transition in $YBa_2Cu_3O_{6.93}$.

In Fig. 2(b), a dI/dV data set for the same field range is shown, but now for a 140 MHz rf current. The average vortex velocity at mode locking, $v = fa$, is therefore over 20 times larger than in Fig. 2(a). Again a clear ML peak is observed at $B = 1.14$ T, but in contrast to the 6 MHz data in (a) the field range in which ML takes place is considerably larger, extending up to $B \simeq 1.3$ T. The nature of the moving medium thus depends strongly on its velocity. For example, at $B = 1.24$ T, one observes liquid

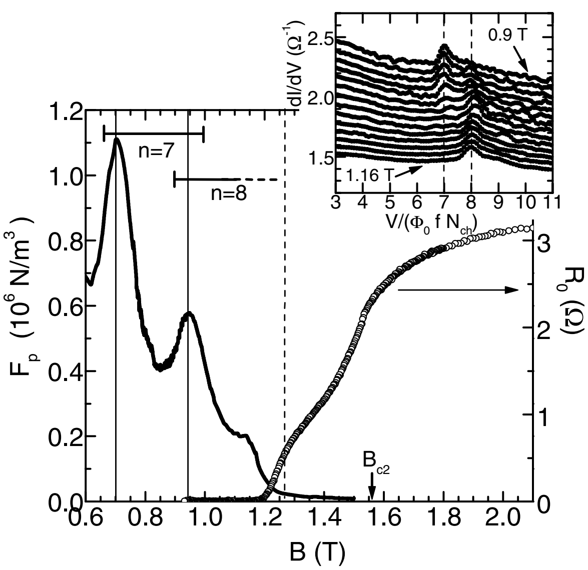

FIG. 1. Shear force density (determined using a velocity criterion $v/a_0 \simeq 1$ MHz) versus field at a temperature $T =$ 1.94 K. Vertical lines indicate the field of the transition from $n = 6 \rightarrow 7$ and $n = 7 \rightarrow 8$, dashed vertical line marks the field where the $n = 8 \rightarrow 9$ transition is expected. Open symbols (right axis): Field dependence of the zero bias resistance R_0. Inset: dI/dV versus normalized voltage in presence of 85 MHz rf currents for $B = 0.9$–1.16 T (steps of 20 mT). The data illustrate the $n = 7 \rightarrow 8$ transition in the ML signal.

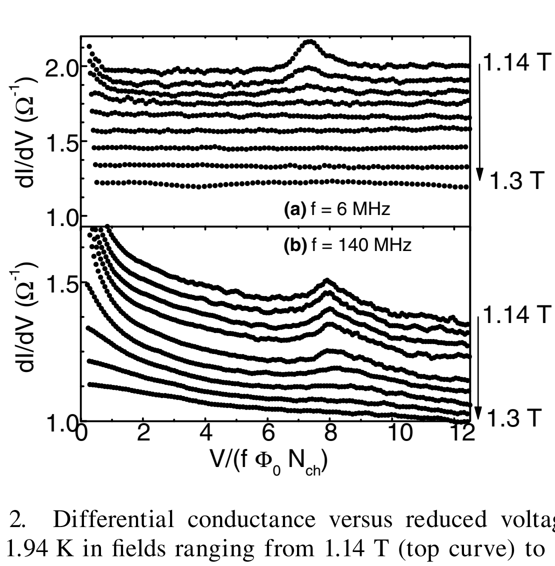

FIG. 2. Differential conductance versus reduced voltage at $T = 1.94$ K in fields ranging from 1.14 T (top curve) to 1.3 T (20 mT steps) for (a) rf current of 6 MHz ($I_{\rm rf} = 0.09$ mA) and (b) 140 MHz and $I_{\rm rf} = 0.94$ mA.

motion for $f = 6$ MHz but coherent motion at 140 MHz. Interestingly, in the early work of Fiory [13], it was already mentioned that the vanishing of the ML signal shifts to larger fields when measured at larger frequency.

For a proper determination of the collapse of the ML signal, we should take into account its dependence on $I_{\rm rf}$ (see, e.g., [21]). Therefore the ML step width ΔI [defined in the inset of Fig. 3(b)] was determined as a function of field for various rf amplitudes and frequencies. The result is shown in Fig. 3(a) for 6 and 60 MHz. As observed, ΔI vanishes linearly with B at a *dynamic melting field* $B_c(f)$ which is essentially independent of $I_{\rm rf}$.

Next we study the frequency dependence of B_c. Rather than plotting B_c versus f, we present the results by plotting the frequency at which ML vanishes, denoted by f_c, versus B, as done in Fig. 3(b). At low fields f_c slowly increases with field, but it starts to diverge at a larger field. Such divergence is expected when we identify $v_c = f_c a$ as the ordering velocity proposed in [5]. In the present case, the plastic (or liquid) flow for $v < v_c$ is controlled by the disordered VLs in the CEs, as we concluded from simulations at small drive (as in [12,19]). This plastic flow involves frequent slip events and transverse vortex jumps between rows. Such behavior has also been observed in magnetic bubble arrays moving along a rough wall [22]. For $v > v_c$, these effects disappear and coherent motion sets in. For $B \gtrsim 1.32$ T, we could no longer resolve the ML effect below 200 MHz. In this field regime, thermal fluctuations alone are sufficient to induce incoherent motion, regardless of the dynamic influence of disorder.

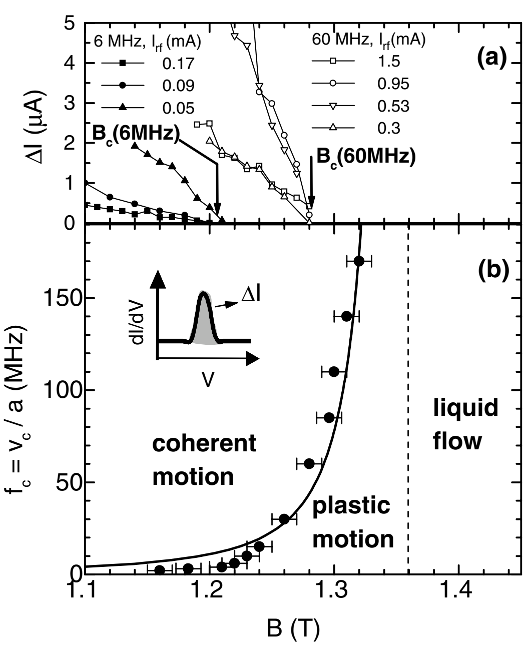

FIG. 3. (a) ML step width ΔI, as defined in the inset of (b), versus field for $f = 6$ MHz and $f = 60$ MHz and several values of $I_{\rm rf}$. Arrows indicate the dynamic field $B_c(f)$. (b) Data points: f_c versus B. Drawn line is a fit according to $f_c \sim (B_{m,e} - B)^{-2}$. The dashed lined marks $B_{m,e} = 1.36$ T.

The $f_c(B)$ data can approximately be fitted to $f_c \sim (B_{m,e} - B)^{-\nu_B}$ with $\nu_B = 2$ and an equilibrium melting field $B_{m,e} = 1.36$ T. An exponent $\nu_B = 1$, as expected from Eq. (1) and the behavior of the melting line, yields a rather poor fit. This discrepancy with the data may originate from the fact that with changing field not only the "distance" $B_{m,e} - B$ to the phase boundary varies, but also the commensurability, i.e., the dislocation density and effective disorder in the channel.

To avoid the possible influence of mismatch and provide a more direct test of Eq. (1), we determined f_c as a function of temperature for $B = 1.16$ T (near matching) from an analysis of the ML amplitude ΔI at several rf currents similar to that in Fig. 3(a) (details are given in [23]). The result is shown in Fig. 4(a). Again a clear divergence of f_c is observed. In this case, the data can be fitted quite well to Eq. (1) written as $f_c = f_0(1 - T/T_{m,e})^{-1}$ with $f_0 = 0.174$ MHz and $T_{m,e} = 2.011$ K. Interestingly, a comparison with the *dc resistance* at various currents [Fig. 4(b)] shows that the equilibrium melting temperature $T_{m,e}$ coincides with the temperature where the $R(T)$ curves merge, i.e., the IV curves become fully linear. This confirms the usual assumption made in dc-transport studies on VL melting [24]. In measurements as a function of field, we observed the merging of $R_{I \leq 1\ \mu A}(B)$ and $R_{I=100\ \mu A}(B)$ at $B \simeq 1.34$ T,

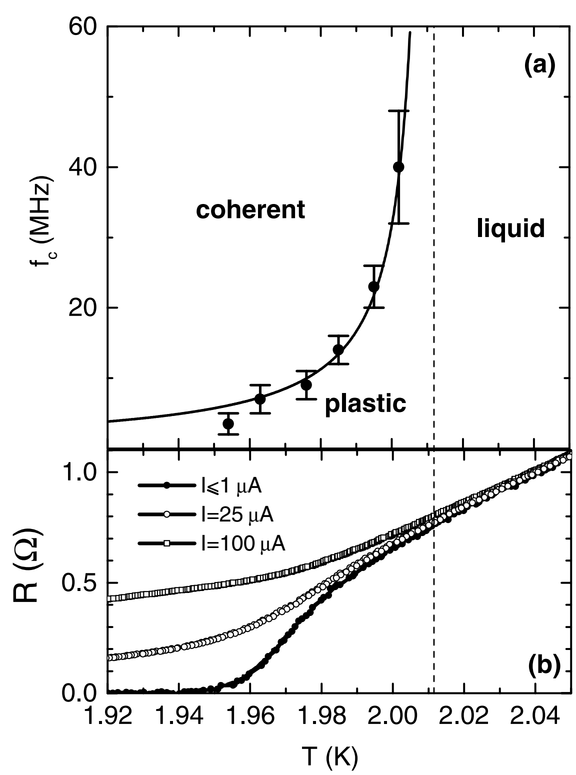

FIG. 4. (a) Data points: Dynamic ordering frequency at $B = 1.16$ T versus temperature. Drawn line: Fit according to $f_c \sim (T_{m,e} - T)^{-1}$ with $T_{m,e} = 2.011$ K (indicated by the dashed line). (b) dc resistance V/I ($I_{\rm rf} = 0$) versus T for several dc currents I.

in good agreement with $B_{m,e}$ determined above. We further note that none of the dc-IV curves show an inflection point, implying that such a feature is not required for microscopic DO [11,25].

It is remarkable that our system, in which "edge disorder" [26] is the prime source of pinning, shows DO typical for a VL with *bulk disorder*. Let us therefore discuss the nature of the DO in more detail. Even for a 2D VL with bulk pinning, the DO was under intensive debate [27–30]. At present, the most likely scenario seems that, on increasing v, after a crossover from fully plastic to partially layered, smectic flow, finally a transition to a moving transverse solid occurs [28]. At this *transverse freezing transition* (TFT), interchain excursions (so-called permeation modes [29]) are suppressed, but free dislocations with Burgers vector parallel to $\vec{v}$ [30] and only longitudinal short-range order (LSRO) remain. Particularly, it is the TFT which is described by T_{sh} [28]. Turning to the channels, we then suggest that our DO boundary $v_c(T, B)$ reflects the TFT in which permeation modes due to roughness of the CE arrays are suppressed. Preliminary simulations support this view [23]. Additionally, above v_c, we observe only *incomplete* ML, suggesting indeed LSRO [29] and residual slip between chains.

The shaking effect in the channels is estimated as follows. The characteristic frequency $f_0 = \Gamma_{p,v}/(k_B T_{m,e} a)$ obtained from Eq. (1), can be derived from Ref. [5] as $f_0 = \sqrt{3/2}\pi\gamma_u \rho_f/(\Phi_0^2 a^2 d k_B T_{m,e})$ with ρ_f the flux flow resistivity, d the film thickness, and γ_u the pinning energy squared times the 2D pinning range. For the channels, the short wavelength ($\sim a_0$) disorder component due to vortex displacements $\mathbf{d}$ in the CE acts in a range $\sim a_0/2$ from the CEs and has a strength $\sim A_s c_{66}$ with $A_s \sim (\sqrt{\langle|\mathbf{d}|^2\rangle}/a_0)/(\pi\sqrt{3})$ [19,23]. We thus assume that "shaking" of the first vortex layer near each CE dominates the TFT. Hence, $\gamma_u \simeq (A_s c_{66} a_0 b_0 d)^2 (a_0/2)^2$. Using the melting criterion $4\pi k_B T_{m,e} \simeq c_{66} a_0^2 d$, one obtains $f_0 \simeq 20 A_s^2 \rho_f k_B T_{m,e}/\Phi_0^2 d$. Taking $\rho_f \simeq \rho_n/2$ and $d = 300$ nm yields $f_0 = A_s^2 \times 500$ MHz. This is in reasonable agreement with the measured value $f_0 = 0.174$ MHz when we assume $A_s \simeq 0.02$, i.e., rms relative displacements in the CE of $(\sqrt{\langle|\mathbf{d}|^2\rangle}/a_0) \simeq 0.1$.

In conclusion, dynamic melting of vortex matter driven through disordered channels was studied by mode-locking experiments. The melting line strongly depends on the ML frequency, i.e., the average velocity. The associated ordering velocity diverges upon approaching the equilibrium melting line, yielding a dynamic phase diagram with coherent, plastic, and fluid flow as predicted theoretically [5,7]. The ML technique presents a powerful tool to study phase transitions in driven periodic media, and we hope our results will stimulate similar investigations in related fields such as CDW dynamics and solid friction.

This work was supported by the Nederlandse Stichting voor Fundamenteel Onderzoek der Materie (FOM).

[1] G. Blatter *et al.*, Rev. Mod. Phys. **66**, 1125, (1994).
[2] G. Grüner, Rev. Mod. Phys. **60**, 1129 (1988).
[3] B. N. J. Persson, *Sliding Friction: Physical Principles and Applications* (Springer-Verlag, Berlin, 1998).
[4] S. Bhattacharya and M. J. Higgins, Phys. Rev. Lett. **70**, 2617 (1993); A. C. Shi and A. J. Berlinsky, Phys. Rev. Lett. **67**, 1926 (1991).
[5] A. E. Koshelev and V. M. Vinokur, Phys. Rev. Lett. **73**, 3580 (1994).
[6] H. J. Jensen *et al.*, Phys. Rev. Lett. **60**, 1676 (1988).
[7] L. Balents and M. P. A Fisher, Phys. Rev. Lett. **75**, 4270 (1995).
[8] M. C. Hellerqvist *et al.*, Phys. Rev. Lett. **76**, 4022 (1996); Phys. Rev. B **56**, 5521 (1997); J. M. E. Geers *et al.*, Phys. Rev. B **63**, 094511 (2001).
[9] S. Ryu *et al.*, Phys. Rev. Lett. **77**, 5114 (1996); M. C. Faleski *et al.*, Phys. Rev. B **54**, 12 427 (1996).
[10] K. E. Bassler *et al.*, Phys. Rev. B **64**, 224517 (2001).
[11] Y. Paltiel *et al.*, Phys. Rev. B **66**, 060503 (2002).
[12] N. Kokubo *et al.*, Phys. Rev. Lett. **88**, 247004 (2002).
[13] A. T. Fiory, Phys. Rev. B **7**, 1881 (1973); A. Schmid and W. Hauger, J. Low Temp. Phys. **11**, 667 (1973).
[14] J. M. Harris *et al.*, Phys. Rev. Lett. **74**, 3684 (1995).
[15] A. B. Kolton *et al.*, Phys. Rev. Lett. **86**, 4112 (2001).
[16] Contrary to usual IV experiments, which cannot distinguish between changes in v or in the fraction of moving vortices, we directly obtain v_c from the ML condition.
[17] M. H. Theunissen *et al.*, Phys. Rev. Lett. **77**, 159 (1996).
[18] R. Besseling *et al.*, Europhys. Lett. **62**, 419 (2003).
[19] R. Besseling, Ph.D. thesis, Leiden University, 2001.
[20] The measurement frequency and dc/rf currents are much smaller than the respective pinning frequency $\omega_p/2\pi = (J_c \rho_f)^{\mathrm{NbN}}/a_0 B \gtrsim 5$ GHz (ρ_f is the flux flow resistivity) and pinning current $J_c \gtrsim 2 \times 10^9$ A/m^2 of the NbN. The CE vortices can therefore be considered as static.
[21] R. E. Thorne *et al.*, Phys. Rev. B **35**, 6360 (1987); Yu. I. Latyshev *et al.*, Phys. Rev. Lett. **87** 247007 (2001).
[22] R. Seshadri and R. M. Westervelt, Phys. Rev. Lett. **70**, 234 (1993); Phys. Rev. B **47**, 8620 (1993).
[23] R. Besseling *et al.* (to be published). See also N. Kokubo *et al.*, cond-mat/0308512.
[24] P. Berghuis *et al.*, Phys. Rev. Lett. **65**, 2583 (1990); Phys. Rev. B **47**, 262 (1993).
[25] A. Duarte *et al.*, Phys. Rev. B **53**, 11 336 (1996).
[26] D. E. Feldman and V. M. Vinokur, Phys. Rev. Lett. **89**, 227204 (2002).
[27] T. Giamarchi and P. Le Doussal, Phys. Rev. Lett. **76**, 3408 (1996); L. Balents *et al.*, Phys. Rev. Lett. **78**, 751 (1997); P. Le Doussal and T. Giamarchi, Phys. Rev. B **57**, 11 356 (1998).
[28] A. B. Kolton *et al.*, Phys. Rev. Lett. **83**, 3061 (1999); Phys. Rev. Lett. **89**, 227001 (2002); S. Scheidl and V. M. Vinokur, Phys. Rev. B **57**, 13 800 (1998).
[29] L. Balents *et al.*, Phys. Rev. B **57**, 7705 (1998).
[30] I. S. Aranson *et al.*, Phys. Rev. B **58**, 14 541 (1998).